Supporting Information

Pt-C Interfaces Based on Electronegativity-Functionalized Hollow Carbon Spheres for Highly Efficient Hydrogen Evolution

Xiao Shang [a], Zi-Zhang Liu [a], Shan-Shan Lu [a], Bin Dong [*a], Jing-Qi Chi [a], Jun-Feng Qin [a], Xien Liu [b], Yong-Ming Chai [a], Chen-Guang Liu [a]

a State Key Laboratory of Heavy Oil Processing, Institute of New Energy, China University of Petroleum (East China), Qingdao 266580, PR China

b College of Chemistry and Molecular Engineering, Qingdao University of Science and Technology, Qingdao 266042, PR China

∗ Corresponding author. Email: dongbin@upc.edu.cn (B. Dong)

Tel: +86-532-86981376, Fax: +86-532-86981787

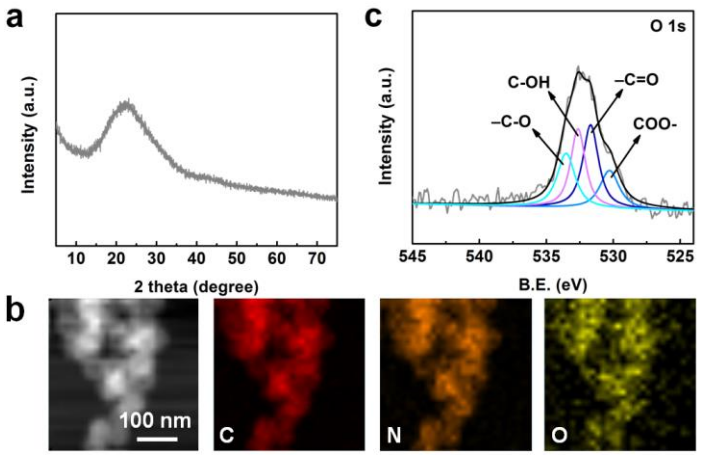

Figure S1 (a) XRD pattern and (b) TEM mapping of HCS. (c) O 1s XPS spectrum of HCS.

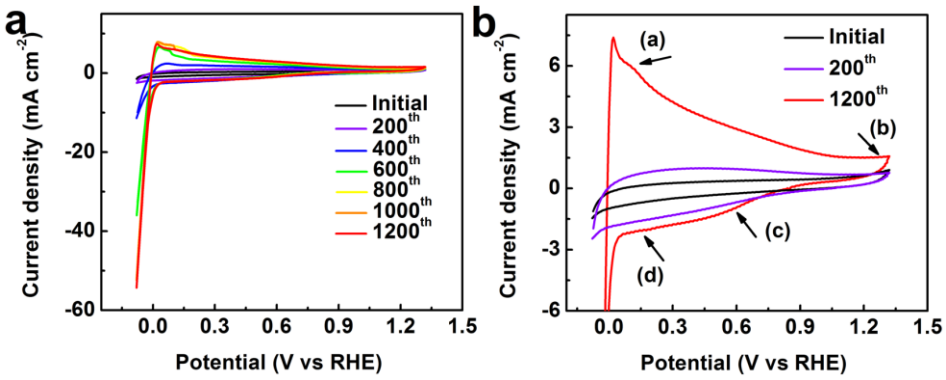

Figure S2 (a) Cyclic voltammogram (CV) and (b) partially magnified area of for electrodissolution access to HCS-Pt.

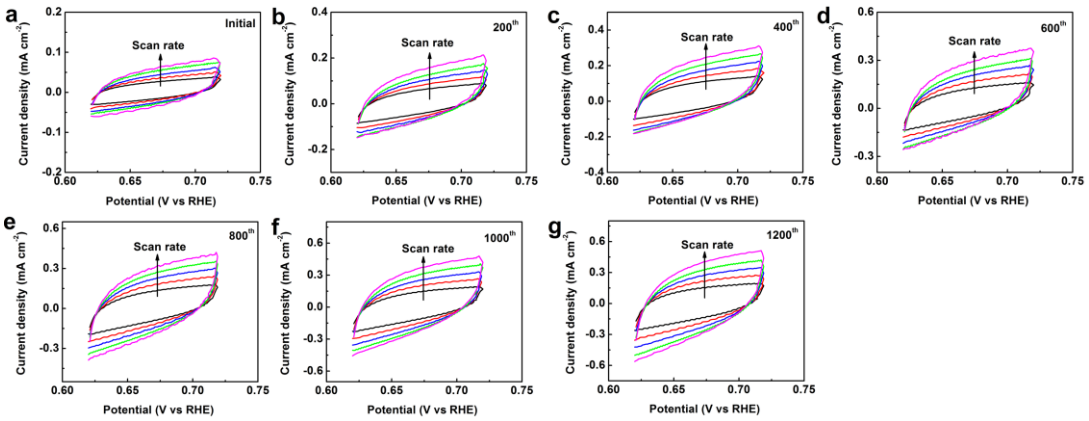

Figure S3 CV measurements for double-layer capacitance (C_{dl}) of HCS-Pt during electrochemical dissolution process varied by different cycles: (a) initial, (b) 200th, (c) 400th, (d) 600th, (e) 800th, (f) 1000th and (g) 1200th.

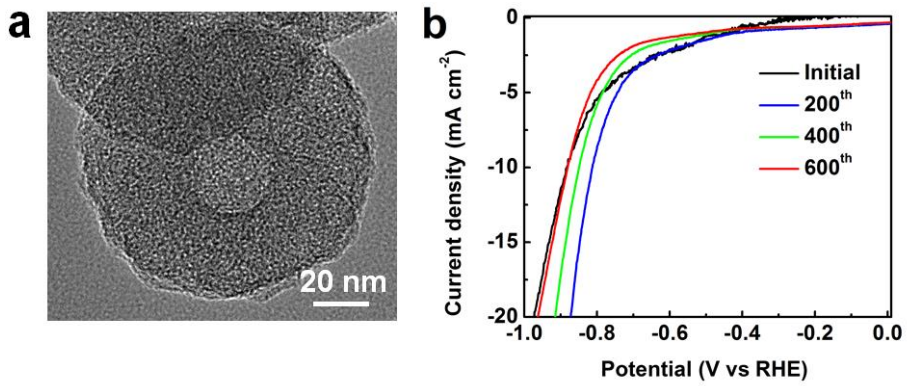

Figure S4 (a) TEM image of HCS-CR and related (b) HER polarization curves.

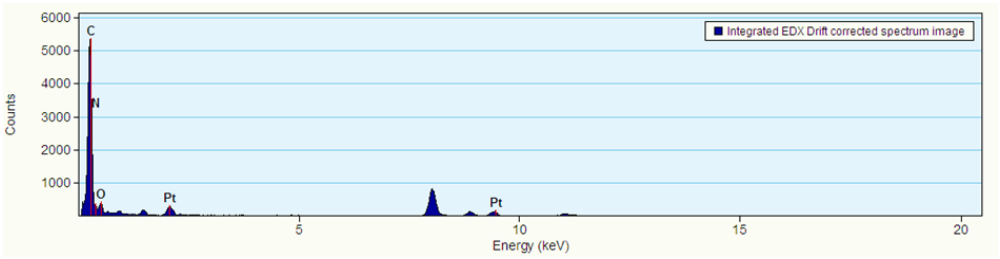

Figure S5 EDX spectrum of HCS-Pt.

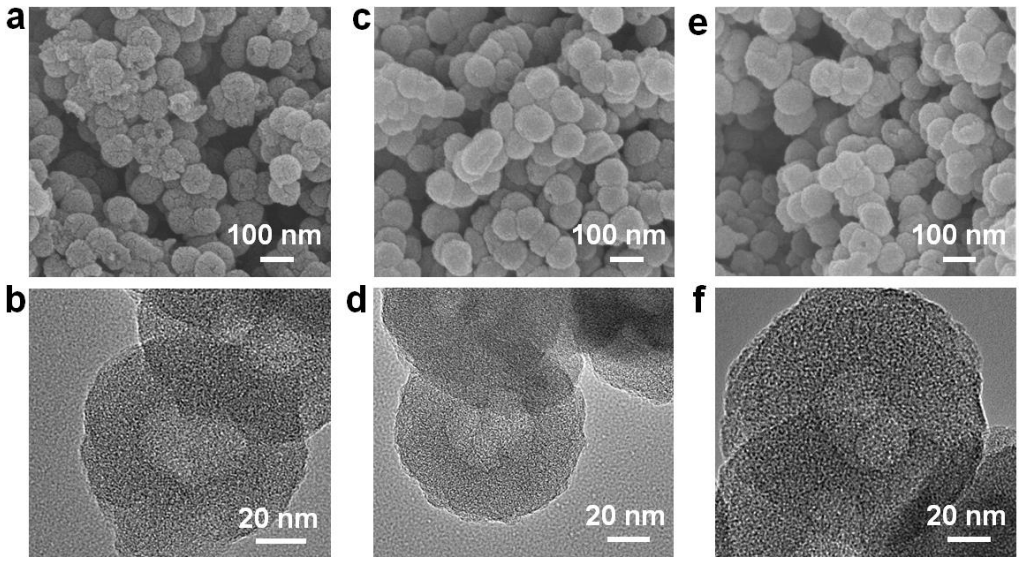

Figure S6 SEM and TEM images of (a, b) HCS-O, (c, d) HCS-N and (e, f) HCS-O-N, respectively.

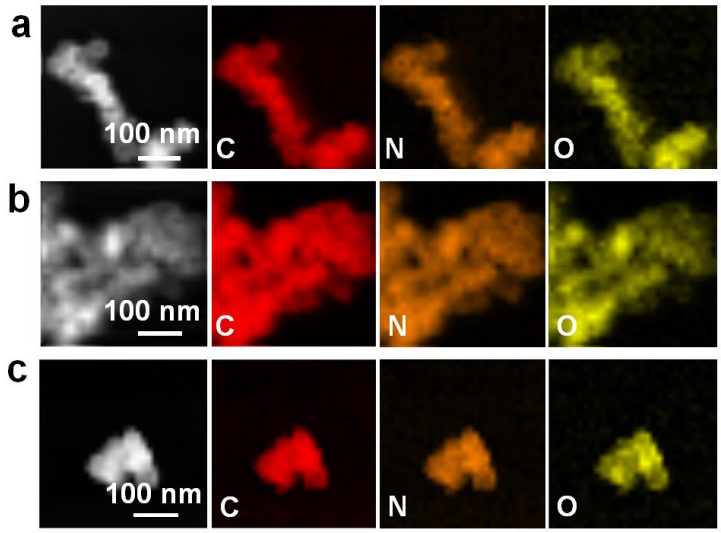

Figure S7 TEM mapping of (a) HCS-O, (b) HCS-N and (c) HCS-O-N.

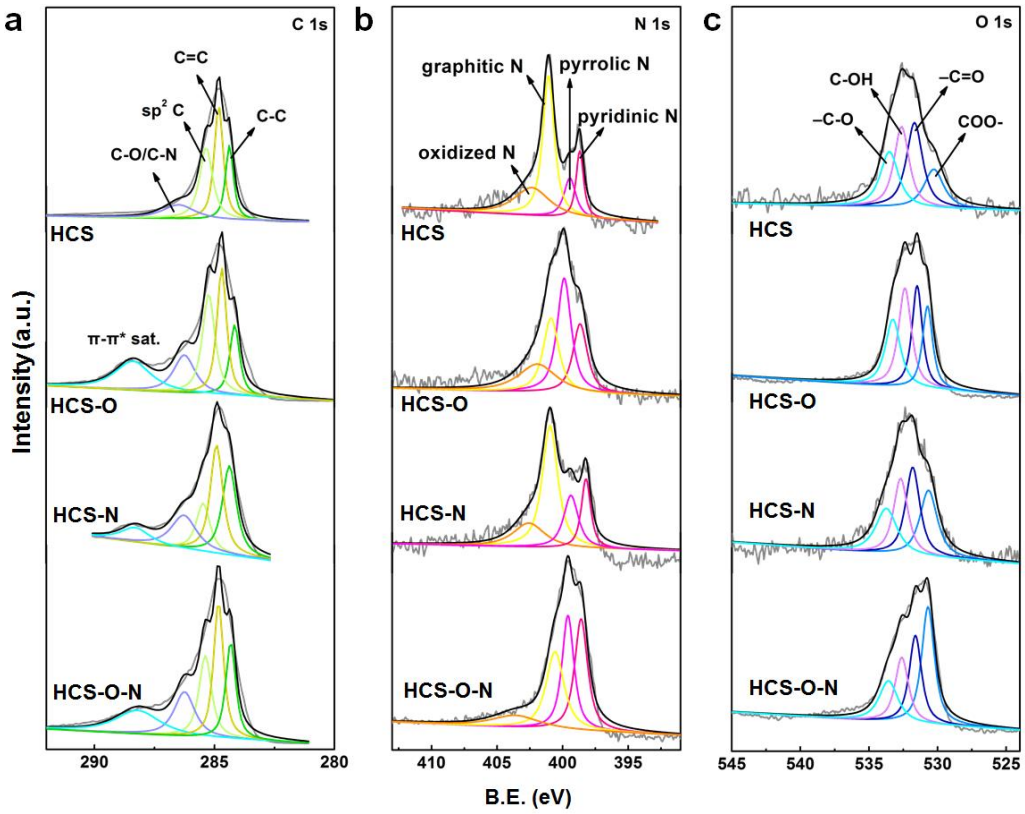

Figure S8 XPS spectra of as-prepared HCS, HCS-O, HCS-N and HCS-O-N: (a) C 1s, (b) N 1s and (c) O 1s.

Table S1 Elemental composition (atomic %) of different carbon substrate obtained from XPS data.

Samples	C	N	O	N/O
HCS	85.57	8.75	5.68	1.53
HCS-O	72.99	6.58	20.43	0.32
HCS-N	83.13	11.05	5.82	1.88
HCS-O-N	85.66	4.44	9.90	0.44

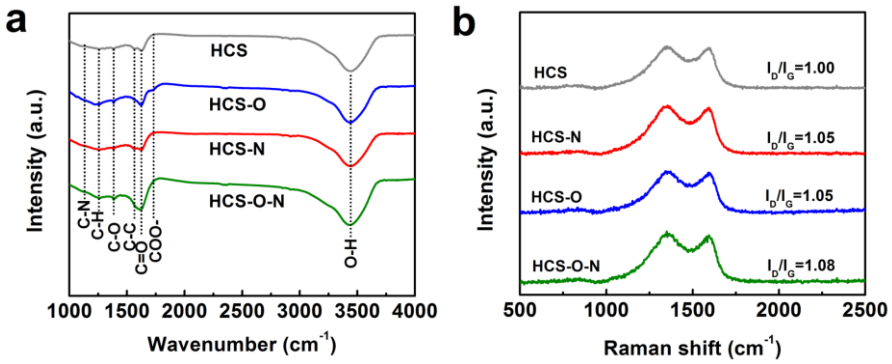

Figure S9 (a) IR and (b) Raman spectra of as-prepared carbon substrates.

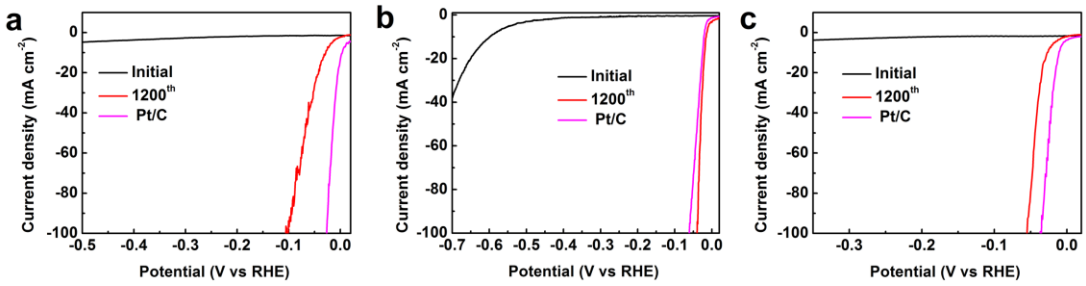

Figure S10 HER activities of (a) HCS-O-Pt, (b) HCS-N-Pt and (c) HCS-O-N-Pt through electrochemical dissolution synthesis.

Figure S11 EDX spectra of (a) HCS-O-Pt, (b) HCS-N-Pt and (c) HCS-O-N-Pt.

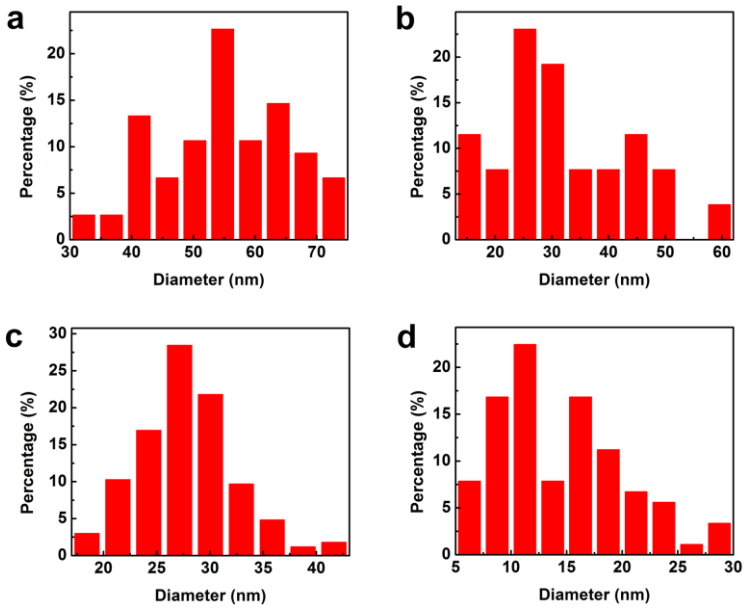

Figure S12 Pt particle size distribution histograms for as-prepared (a) HCS-Pt, (b) HCS-O-Pt, (c) HCS-N-Pt and (d) HCS-O-N-Pt.

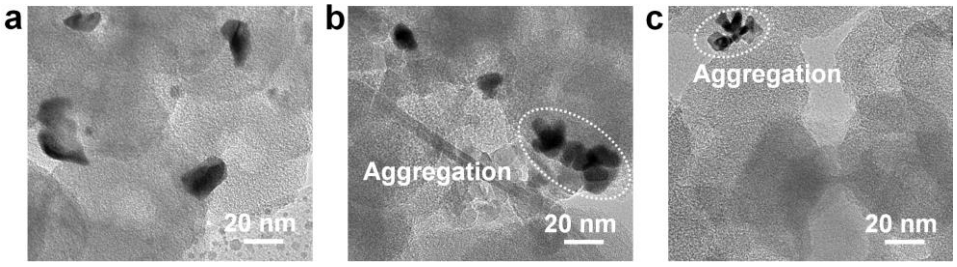

Figure S13 TEM images of (a) HCS-N-Pt, (b) HCS-O and (c) HCS-O-N-Pt.

Table S2 Pt contents on various carbon substrates by ICP-OES.

Samples	Pt (μg cm^{-2})
HCS-Pt	1.0
HCS-O-Pt	6.2
HCS-N-Pt	1.7
HCS-O-N-Pt	2.3

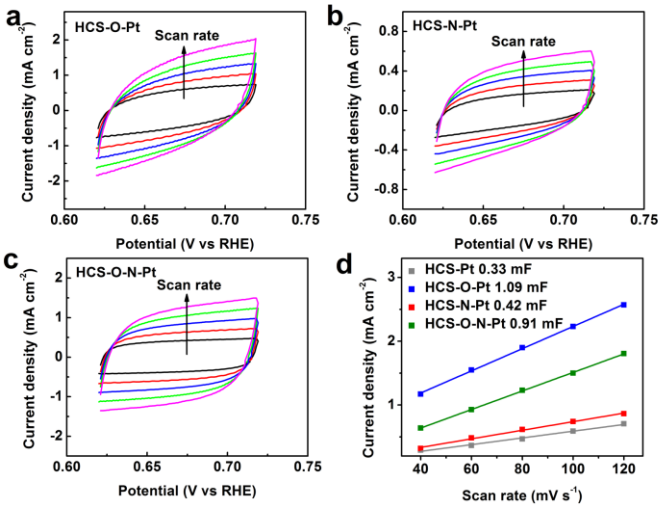

Figure S14 CV measurements for C_{dl} of (a) HCS-O-Pt, (b) HCS-N-Pt and (c) HCS-O-N-Pt. (d) Determined C_{dl} of the above catalysts.

Table S3 Calculated C_{dl} and ECSA values of catalysts.

Sample	C_{dl}, mF	C_s, mF cm^{-2}	ECSA, cm^2	GSA, cm^2	RF
HCS-Pt	0.33	0.035	9.43	0.1256	75.07
HCS-O-Pt	1.09	0.035	31.14	0.1256	247.95
HCS-N-Pt	0.42	0.035	12.00	0.1256	95.54
HCS-O-N-Pt	0.91	0.035	26.00	0.1256	207.01

Calculation of turnover frequency (TOF)

The absolute components of voltammetric charges (cathodic and anodic) can be obtained from the CV curves from -0.2 V to 0.6 V (vs RHE) in pH=7 phosphate buffer solution (PBS) as shown in Figure S14. The value of TOF can be determined by the following equations: [1-3]

$$n = Q/2F \quad (1)$$

$$TOF = I/2Fn \quad (2)$$

n: the number of active sites (mol).

Q: the number of voltammetric charges (C);

F: Faraday constant (96500 C mol^{-1}).

I: current (A) in the linear sweep measurement;

The factor of 1/2 in the eq (4) represents that two electrons are needed to form one hydrogen molecule from two protons.

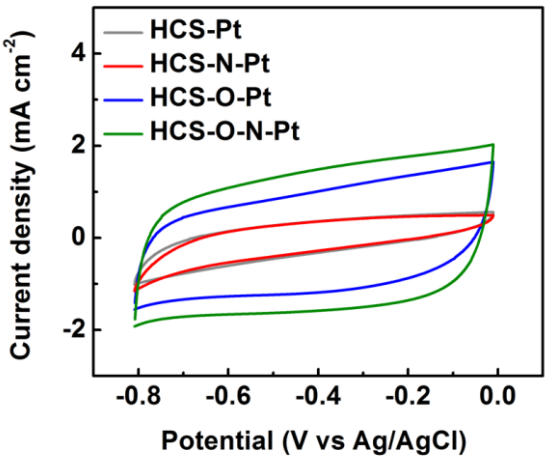

Figure S15 CVs of as-prepared samples in pH=7 phosphate buffer solution at a scan rate of 50 mV s^{-1}.

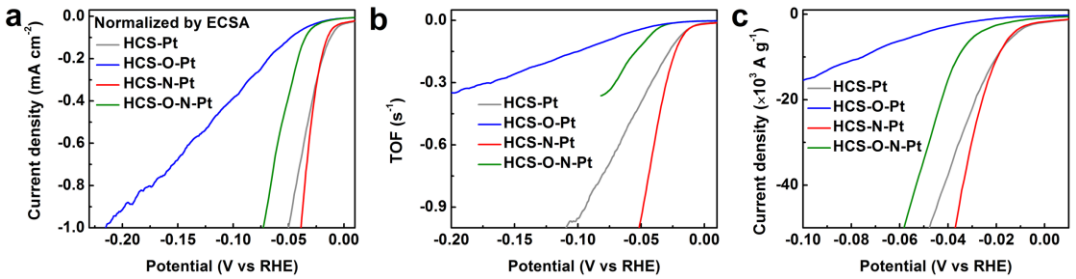

Figure S16 Comparison of HER activities among HCS-Pt, HCS-O-Pt, HCS-N-Pt and HCS-O-N-Pt: (a) LSV curves normalized by ECSA and (b) TOF and (c) mass activity based on Pt loading in Table S2.

Table S4 Comparison of HER activities for Pt-based electrocatalysts in recent work.

Sample	Electrolyte	Overpotential η at 10 mA cm^{-2} (mV)	Overpotential η at 100 mA cm^{-2} (mV)	Current density j (mA cm^{-2})	Overpotential η at j (mV)	Tafel slope (mV dec^{-1})	Ref.
Pt doped MoS_2	0.5 M H_2SO_4	150	-	-	-	96	[4]
Pt@NHPCP	0.1 M $HClO_4$	57	-	-	-	27	[5]
Pt/MoS_2	0.1 M H_2SO_4	86	-	91.5	300	52	[6]
CTNC-700pt	0.5 M H_2SO_4	-	-	-	-	28	[7]
A-CN(PDAP)*	0.5 M H_2SO_4	-	-	60	50	-	[8]
Pt/amino-rGO	0.5 M H_2SO_4	-	-	35.5	90	26	[9]
400-SWNT/Pt	0.5 M H_2SO_4	27	130	180	210	38	[10]
GO/DenPtNPs	0.5 M H_2SO_4	-	-	0.4	50	58	[11]
Pt/MoS_2/CC	0.5 M H_2SO_4	18	-	-	-	49	[12]
Pt@Pd NFs/rGO	0.5 M H_2SO_4	56	-	-	-	39	[13]
polyTT-Pt	0.5 M H_2SO_4	67	-	-	-	37	[14]
Pt200-VGNSAs/CC	0.5 M H_2SO_4	60	-	-	-	28.5	[15]
Pt/CFC	0.5 M H_2SO_4	4.5	34.5	170	43.5	-	[16]
HCS-N-Pt	0.5 M H_2SO_4	14.4	40	342	100	22	**This work**

* without iR correction

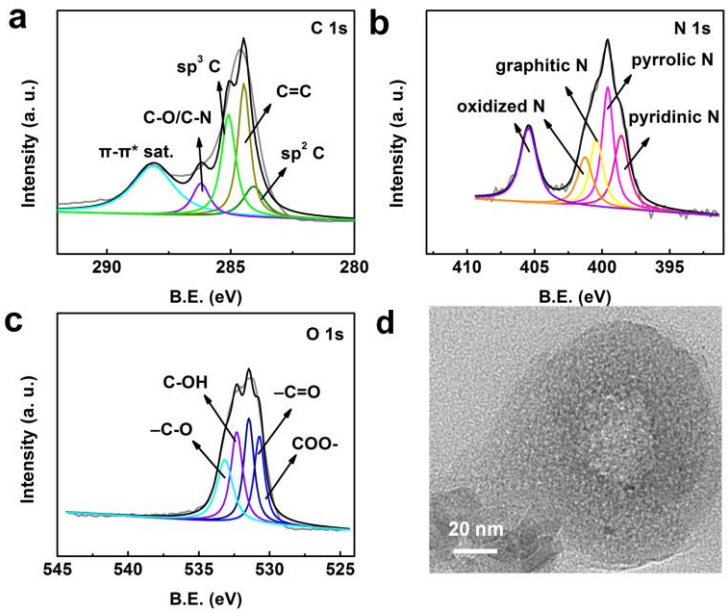

Figure S17 XPS spectra of HCS-O2: (a) C 1s, (b) N 1s and (c) O 1s. (d) TEM image of HCS-O2.

Table S5 Elemental contents of HCS-O2 by XPS.

Sample	C (atomic %)	N (atomic %)	O (atomic %)	N/O
HCS-O2	66.98	7.09	25.92	0.27

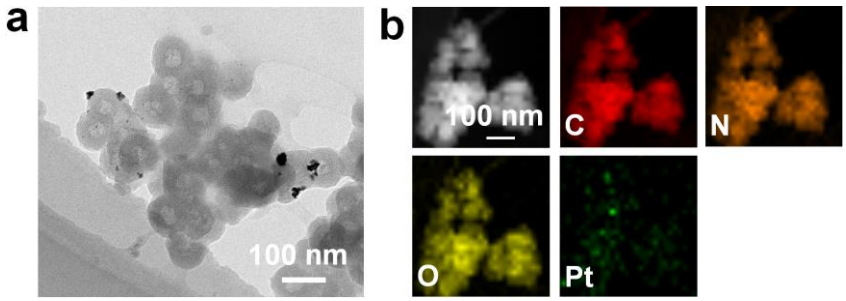

Figure S18 (a) TEM and (b) TEM mapping of HCS-O2-Pt.

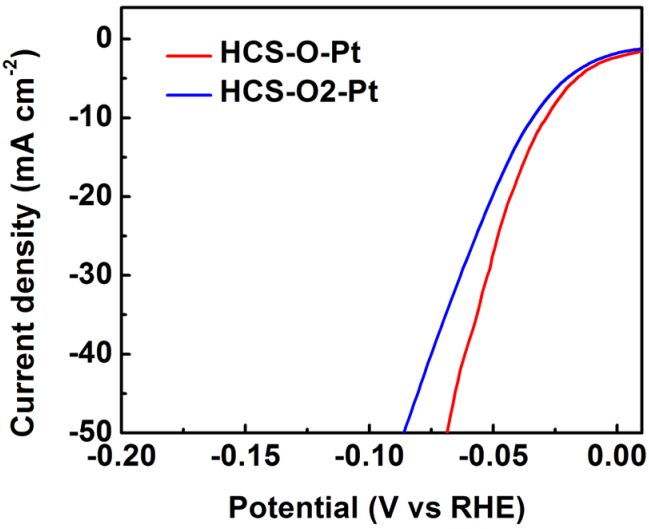

Figure S19 LSV curves of HCS-O2-Pt compared with HCS-O-Pt.

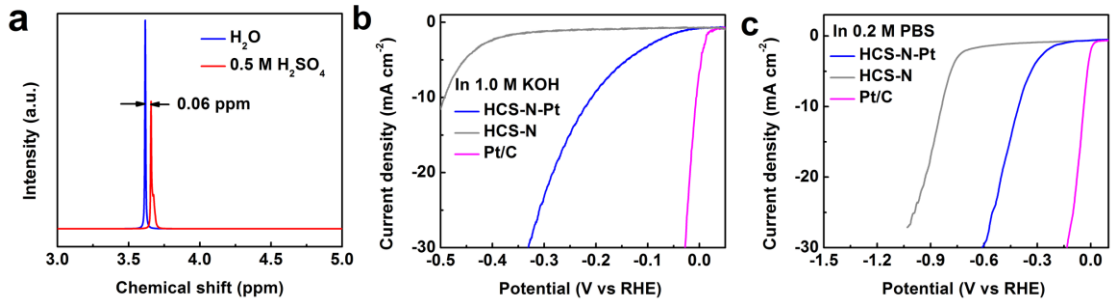

Figure S20 (a) ^{1}H NMR spectra of 0.5 M H_2SO_4 and deionized water. HER activities of HCS-N-Pt and Pt/C in (b) alkaline (1.0 M KOH) and (c) 0.2 M phosphate buffer solution (PBS).

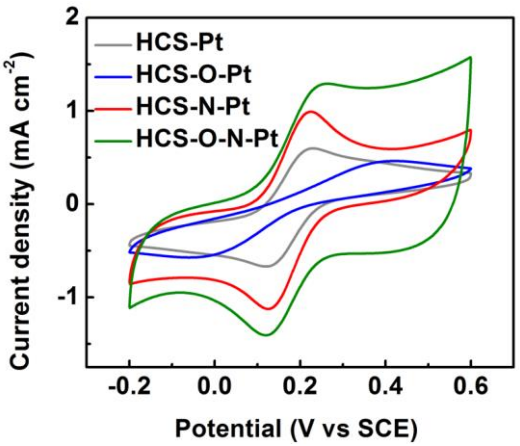

Figure S21 Heterogeneous electron transfer (HET) rate by CV (scan rate of 100 mV s^{-1}) in the electrolyte containing $K_3[Fe(CN)_6]$ (5 mM) and KCl (0.1 M).

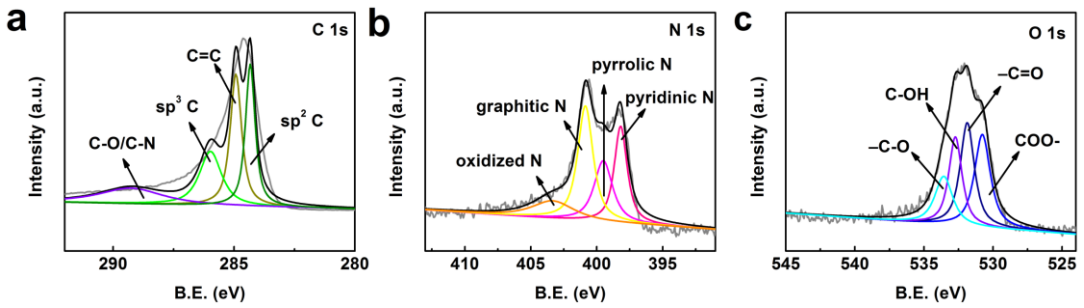

Figure S22 XPS spectra of HCS-N with nitriding time of 6 h: (a) C 1s, (b) N 1s and (c) O 1s.

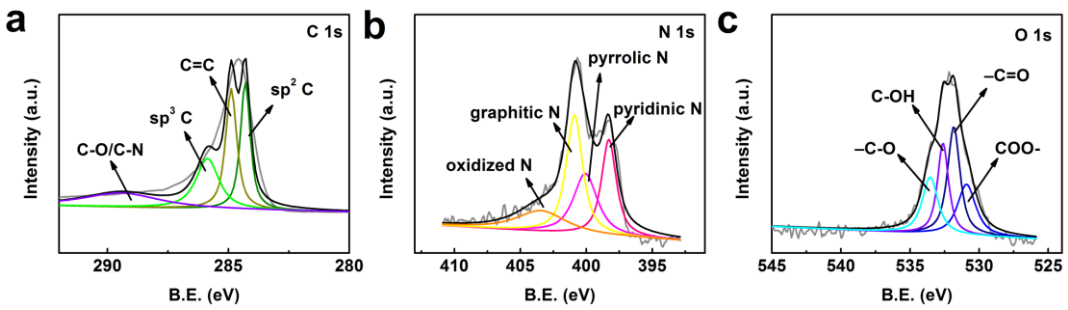

Figure S23 XPS spectra of HCS-N with nitriding time of 24 h: (a) C 1s, (b) N 1s and (c) O 1s.

Table S6 Elemental composition of carbon substrates varied by different nitriding time obtained from XPS data.

Nitriding time	C (atomic %)	N (atomic %)	O (atomic %)	N/O
6 h	86.08	8.26	5.65	1.47
12 h	83.13	11.05	5.82	1.88
24 h	88.49	6.59	4.92	1.33

Table S7 ICP-OES data of Pt content on HCS-N varied by nitriding time.

Nidriding time	Pt (μg cm^{-2})
6 h	0.8
12 h	1.7
24 h	0.2

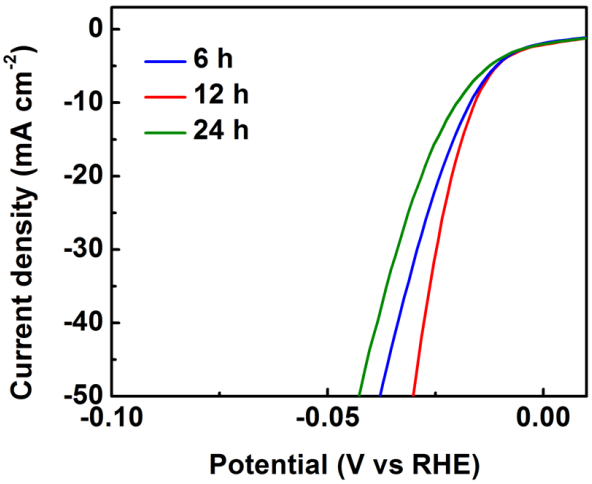

Figure S24 HER activity of HCS-N-Pt with substrate under different nidriding time (6 h, 12 h and 24 h) in 0.5 M H_2SO_4.

Table S8 ICP-OES data of Pt content on HCS-N by different deposition cycles.

Number of cycles	Pt (μg cm^{-2})
800 cycles	0.12
1200 cycles	1.70
1400 cycles	1.83

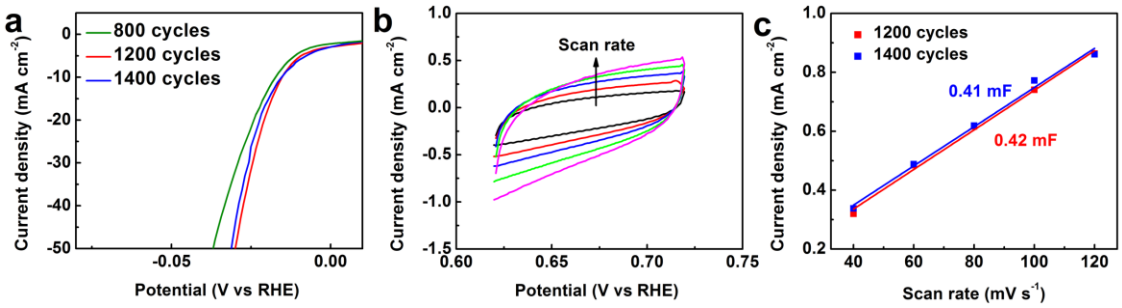

Figure S25 (a) LSV curves of HCS-N-Pt for 800, 1200 and 1400 cycles. (b) CV measurements for C_{dl} of HCS-N-Pt deposited for 1400 cycles. (c) Determined C_{dl} of HCS-N-Pt deposited for 1200 and 1400 cycles.

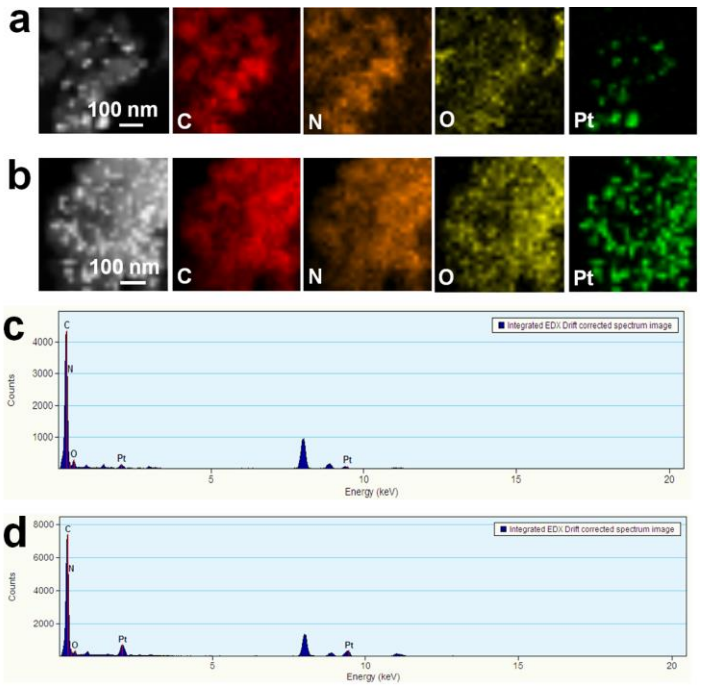

Figure S26 TEM mapping and EDX spectra of HCS-N-Pt after (a, c) i-t of 12 h and (b, d) CV for 5000 cycles.

REFERENCES

(1) Benck, J. D.; Chen, Z.; Kuritzky, L. Y.; Forman, A. J.; Jaramillo, T. F. Amorphous Molybdenum Sulfide Catalysts for Electrochemical Hydrogen Production: Insights into the Origin of Their Catalytic Activity. *ACS Catal.* **2012**, *2*, 1916-1923.

(2) Mccrory, C. C.; Jung, S.; Peters, J. C.; Jaramillo, T. F. Benchmarking Heterogeneous Electrocatalysts for the Oxygen Evolution Reaction. *J. Am. Chem. Soc.* **2013**, *135*, 16977-16987.

(3) Chen, Z.; Cummins, D.; Reinecke, B. N.; Clark, E.; Sunkara, M. K.; Jaramillo, T. F. Core-Shell MoO_3-MoS_2 Nanowires for Hydrogen Evolution: a Functional Design for Electrocatalytic Materials. *Nano Lett.* **2011**, *11*, 4168-4175.

(4) Deng, J.; Li, H.; Xiao, J.; Tu, Y.; Deng, D.; Yang, H.; Tian, H.; Li, J.; Ren, P.; Bao, X. Triggering the Electrocatalytic Hydrogen Evolution Activity of the Inert Two-Dimensional MoS_2 Surface via Single-Atom Metal Doping. *Energy Environ. Sci.* **2015**, *8*, 1594-1601.

(5) Ying, J.; Jiang, G.; Paul Cano, Z.; Han, L.; Yang, X.-Y.; Chen, Z. Nitrogen-Doped Hollow Porous Carbon Polyhedrons Embedded with Highly Dispersed Pt Nanoparticles as a Highly Efficient and Stable Hydrogen Evolution Electrocatalyst. *Nano Energy* **2017**, *40*, 88-94.

(6) Ren, W.; Zhang, H.; Cheng, C. Ultrafine Pt Nanoparticles Decorated MoS_2 Nanosheets with Significantly Improved Hydrogen Evolution Activity. *Electrochim. Acta* **2017**, *241*, 316-322.

(7) Gottlieb, E.; Kopeć, M.; Banerjee, M.; Mohin, J.; Yaron, D.; Matyjaszewski, K.;

Kowalewski, T. In-Situ Platinum Deposition on Nitrogen-Doped Carbon Films as a Source of Catalytic Activity in a Hydrogen Evolution Reaction. *ACS Appl. Mater. Interfaces* **2016**, *8*, 21531-21538.

(8) Ji, L.; Wang, J.; Zuo, S.; Chen, Z. In Situ Preparation of Pt Nanoparticles Supported on N-Doped Carbon as Highly Efficient Electrocatalysts for Hydrogen Production. *J. Phys. Chem. C* **2017**, *121*, 8923-8930.

(9) Navaee, A.; Salimi, A. Anodic Platinum Dissolution, Entrapping by Amine Functionalized-Reduced Graphene Oxide: a Simple Approach to Derive the Uniform Distribution of Platinum Nanoparticles with Efficient Electrocatalytic Activity for Durable Hydrogen Evolution and Ethanol Oxidation. *Electrochim. Acta* **2016**, *211*, 322-330.

(10) Tavakkoli, M.; Holmberg, N.; Kronberg, R.; Jiang, H.; Sainio, J.; Kauppinen, E. I.; Kallio, T.; Laasonen, K. Electrochemical Activation of Single-Walled Carbon Nanotubes with Pseudo-Atomic-Scale Platinum for the Hydrogen Evolution Reaction. *ACS Catal.* **2017**, *7*, 3121-3130.

(11) Devadas, B.; Imae, T. Hydrogen Evolution Reaction Efficiency by Low Loading of Platinum Nanoparticles Protected by Dendrimers on Carbon Materials. *Electrochem. Commun.* **2016**, *72*, 135-139.

(12) Luo, Y.; Huang, D.; Li, M.; Xiao, X.; Shi, W.; Wang, M.; Su, J.; Shen, Y. MoS_2 Nanosheet Decorated with Trace Loads of Pt as Highly Active Electrocatalyst for Hydrogen Evolution Reaction. *Electrochim. Acta* **2016**, *219*, 187-193.

(13) Lin, X.-X.; Wang, A.-J.; Fang, K.-M.; Yuan, J.; Feng, J.-J. One-Pot Seedless

Aqueous Synthesis of Reduced Graphene Oxide (rGO)-Supported Core-Shell Pt@Pd Nanoflowers as Advanced Catalysts for Oxygen Reduction and Hydrogen Evolution. *ACS Sustain. Chem. Eng.* **2017**, *5*, 8675-8683.

(14) Chakrabartty, S.; Gopinath, C. S.; Raj, C. R. Polymer-Based Hybrid Catalyst of Low Pt Content for Electrochemical Hydrogen Evolution. *Int. J. Hydrogen Energy* **2017**, *42*, 22821-22829.

(15) Zhang, H.; Ren, W.; Guan, C.; Cheng, C. Pt Decorated 3D Vertical Graphene Nanosheet Arrays for Efficient Methanol Oxidation and Hydrogen Evolution Reaction. *J. Mater. Chem. A* **2017**, 22004-22011.

(16) Wu, T.; Wang, G.; Zhang, Y.; Kang, S.; Zhang, H. Electrochemical Deposition of Pt on Carbon Fiber Cloth Utilizing Pt Mesh Counter Electrode during Hydrogen Evolution Reaction for Electrocatalytic Hydrogenation Reduction of p-Nitrophenol. *New J. Chem.* **2017**, *41*, 7012-7019.